DOI: 10.22499/3.6901.001

JSHESS early online view

Optical Properties of Sydney Aerosols

Gail P. Box[1] and Taleb Hallal [1,2]

[1] University of New South Wales, Sydney, Australia
[2] Boral Cement, Sydney, Australia

(Manuscript received July 2018; accepted January2019)

Aerosol chemistry for $PM_{2.5}$ and PM_{10} (particulate matter less than 2.5 and 10-μm aerodynamic diameter) samples collected in the Sydney region between November 2002 and December 2003 has been used to estimate size-resolved refractive index for Sydney. Seasonal $PM_{10\text{-}2.5}$ chemistry was obtained by subtracting seasonal $PM_{2.5}$ from seasonal PM_{10} chemical composition. The chemical compounds present were determined from the elemental composition using two methods: the SCAPE 2 chemical thermodynamic model; and aerosol types based on marker elements. Refractive index was then calculated using a mass fraction approach. Both methods agreed within the error bars indicating that useful optical properties can be derived from elemental chemistry. For the fine mode ($PM_{2.5}$) the real component of the refractive index was 1.46 ± 0.07 with no seasonal variation, but there were seasonal variations in imaginary component, 0.05 ± 0.02 in summer and 0.23 ± 0.05 in spring. The coarse mode ($PM_{10\text{-}2.5}$) real refractive index was constant throughout the year at 1.47 ± 0.09 while the imaginary refractive index was 0.01 ± 0.04 in summer and 0.04 ± 0.06 in spring. Representative refractive indices were then used to calculate aerosol scattering properties for three different size distributions to illustrate how this information could be used.

1 Introduction

Sunlight passing through the atmosphere is scattered and absorbed by the clouds, molecules and particles in the atmosphere. Scattering by molecules is responsible for the blue colour of the sky and the red of sunset. Scattering by clouds reduces incoming sunlight and makes cloudy days cooler. Scattering by aerosol particles is responsible for hazy days, especially in industrialized regions, as well as other subtle effects which can impact on climate from the regional to the global level. Scattering and absorption by aerosol particles can affect visibility in some regions and must be taken into account when considering radiative forcing and climate impacts. To quantify effects such as visibility and radiative forcing we need to know the aerosol optical properties such as the refractive index, scattering coefficient, absorption coefficient and asymmetry parameter. Aerosol refractive index is strongly dependent on aerosol chemistry while scattering coefficient, absorption coefficient and asymmetry parameter depend on both refractive index and aerosol size distribution. Aerosols are ubiquitous in the atmosphere but are highly variable in space and time, so local and regional knowledge of their properties is needed in order to evaluate their effects on air quality, health, and their climate impacts such as radiative forcing for the particular region.

Aerosol chemical composition varies with location, for example between urban and rural areas, between coastal and inland regions. It can also vary with season: for example the sea salt component on the coast will be affected by seasonal variations in on-shore winds; black carbon (BC) from motor vehicles and fossil fuel burning may be elevated in winter due to domestic heating. Sea salt affects the scattering of light whereas black carbon primarily affects absorption.

Corresponding author: <<Gail Box>>, <School of Physics, University of New South Wales, Sydney, NSW 2052 Australia>>
Email: <<gailpbox@gmail.com>>

It is beyond the scope of this paper to provide an overview of methods used to determine aerosol scattering and absorption properties. Hand and Malm (2007) provide a review of ground-based measurements of aerosol scattering, while reviews of absorption measurements are given in Horvath (1993) and Bond and Bergstrom (2006). The focus of this paper is aerosol refractive index with the real part which is related to scattering, and the imaginary part which is related to absorption, treated separately.

Between November 2002 and December 2003 samples of $PM_{2.5}$ and PM_{10} (particulate matter less than 2.5 and 10-μm aerodynamic diameter) aerosols were collected at four sites in the greater Sydney Basin. The objectives of this study were firstly to determine the spatial and seasonal variation of size-resolved aerosol chemical composition in the Sydney region (Halal et al., 2013), and secondly to use the aerosol chemistry to determine aerosol refractive index for this region. This paper focuses on the second of these objectives, the determination of refractive index. Thence optical properties such as extinction efficiency, scattering and absorption efficiency, single scattering albedo and asymmetry parameter can be calculated.

Aerosol refractive index was determined from elemental chemistry using two methods: a chemical thermodynamic model and aerosol types. Refractive index was then determined for $PM_{2.5}$, PM_{10} and $PM_{10\text{-}2.5}$ (particulate matter between 2.5-μm and 10-μm aerodynamic diameter) size fractions, and their seasonal and spatial variations examined. Representative values of refractive index were then used with three different aerosol size distributions representative of Sydney to examine how aerosol extinction, asymmetry parameter and single scattering albedo vary with season and aerosol size distribution.

2 Methodology

2.1 Sample collection and analysis

A detailed description of the sampling and analysis for this study is given in Hallal et al. (2013) so only a brief outline is provided here. Sampling was carried out at four sites: Kensington, an urban area; Campbelltown, a semi-urban area; Moss Vale, a rural-urban area; and Berrima, a rural-industrial area (major cement plant and stock-feed mill). Kensington is close to both the coast and the Sydney central business district (CBD); Campbelltown is 45 km south-west of the Sydney CBD; Moss Vale and Berrima are both in the Southern Highlands south of Sydney, 140km and 130 km respectively from the Sydney CBD. These sites represent the different environmental, topographic and meteorological conditions in the Sydney region.

A total of 102 samples were collected on several days at each site in summer, autumn, winter and spring using an Ecotech MicroVol 1000 sampler with a flow rate of 3 litre/minute. The samples were collected on 47mm Nuclepore Polycarbonate Membrane Filters with a 1.0 μm pore size. Most samples were collected over a 24 hour period, and on most days a $PM_{2.5}$ and a PM_{10} (particulate matter less than 2.5-μm and 10-μm aerodynamic diameter) sampler were run side by side in order to identify size-related differences in composition.

The elemental composition of the samples was determined using the accelerator-based Ion Beam Analysis (IBA) techniques Proton-Induced X-Ray Emission (PIXE) and Proton-Induced Gamma-ray Emission (PIGE) (Cohen et al., 2004) at the Australian Nuclear Science and Technology Organisation (ANSTO). Black carbon (BC) was determined using the Laser Integrating Plate Method (Taha et al., 2007).

2.2 Determination of Chemical Composition

In order to determine the refractive index of the atmospheric aerosol it is necessary to know which compounds are present in the air. Two methods have been applied to the elemental composition data to determine the chemical compounds present. The simplest method uses marker elements to determine aerosol types. The second method is a chemical thermodynamic model which uses ionic composition and thus required some assumptions to be made. Both methods are described below.

2.2.1 Aerosol Types

In Hallal et al. (2013) elemental chemistry was used to determine typical aerosol types, based on Malm et al. (1994). It would also be suited to large data sets and ongoing monitoring.

Aerosols can be classified into a number of major types: sea salt, sulfates, nitrates, soil, organics and light-absorbing carbon (Malm et al., 1994). For each aerosol type the elemental concentration of its marker element is multiplied by a scaling factor obtained by dividing the total molar weight of the aerosol type by the atomic weight of the marker element. The type definitions used are given below.

Sea salt = 2.54*[Na]

Soil = 2.2*[Al] + 2.49*[Si] + 1.63*[Ca] + 1.94*[Ti] + 2.42*[Fe]

Sulphate = 4.125*[S]

Smoke = [K] – 0.6*[Fe]

Square brackets in the above equations indicate element concentrations. Sulfate was assumed to be fully neutralised and found as $(NH_4)_2SO_4$. Black carbon (also called light absorbing carbon) was found using the Laser Integrating Plate Method (Taha et al. 2007). Since no measurements of O, H or N were available for this study [water + nitrates] was assumed to be 16% of total mass (Cohen et al., 1995). Organic was then estimated as:

Organic = Measured mass – Sea salt – Soil – Sulphate – Smoke - BC – [water + nitrates]

For each sample the mass of each aerosol type was calculated from the measured elemental composition and from this the percentage of total sample mass accounted for by each aerosol type was obtained.

The summer and winter average $PM_{2.5}$ and PM_{10} aerosol composition for each site are illustrated in Figure 1. It is evident that there are seasonal variations in aerosol composition. Sea salt and sulfate account for a higher fraction of total aerosol in summer (lefthand panel) than in winter (righthand panel) for both $PM_{2.5}$ (top row) and PM_{10} (bottom row). For black carbon there are distinct seasonal variations for all sites and it accounts for a greater fraction of $PM_{2.5}$ than PM_{10}. More detailed discussion of aerosol types is given in Hallal et al. (2013).

2.2.2 Thermodynamic model

The SCAPE 2 chemical equilibrium thermodynamic model (Kim et al., 1993a and 1993b; Kim and Seinfeld 1995, Meng et al., 1995) was used to estimate the state and composition of inorganic species in the aerosol phase. The model assumes a system of ammonium, chloride, nitrate, sodium, sulfate, calcium, potassium, magnesium and carbonate ions and water which exists in solid and liquid phases. Given the concentration of the respective ions for a mixture of water-soluble inorganic particles, relative humidity (RH) and temperature as an input, the model calculates the equilibrium physical state and composition of the mixture. For the current study the program returned mass concentration of ions and compounds present at ambient temperature and relative humidity. The necessity of assuming equivalence between ionic and elemental composition is a source of error. Errors are discussed below after discussion of refractive index calculations.

The model was run for each $PM_{2.5}$ and PM_{10} sample (daily mass) as well as for seasonal and year average $PM_{2.5}$ and PM_{10} (average mass) at each site. Since a major focus of this work was to obtain size-resolved optical properties, coarse mode elemental composition ($PM_{10\text{-}2.5}$) was determined by subtracting seasonally averaged $PM_{2.5}$ from seasonally averaged PM_{10} concentrations. These values were then used as input to SCAPE 2.

The output from SCAPE 2 represents the soluble component of the aerosol. Black carbon and soil were as defined above. Organic mass was then determined by subtracting soluble mass, soil and black carbon from total mass.

2.3 Determination of aerosol refractive index

Aerosol refractive index was calculated using a mass fraction approach. Refractive index, n, is given by:

$$n = \sum (m_i \, n_i) / M$$

Here m_i is the mass of the ith compound, n_i is its refractive index and M is total sample mass.

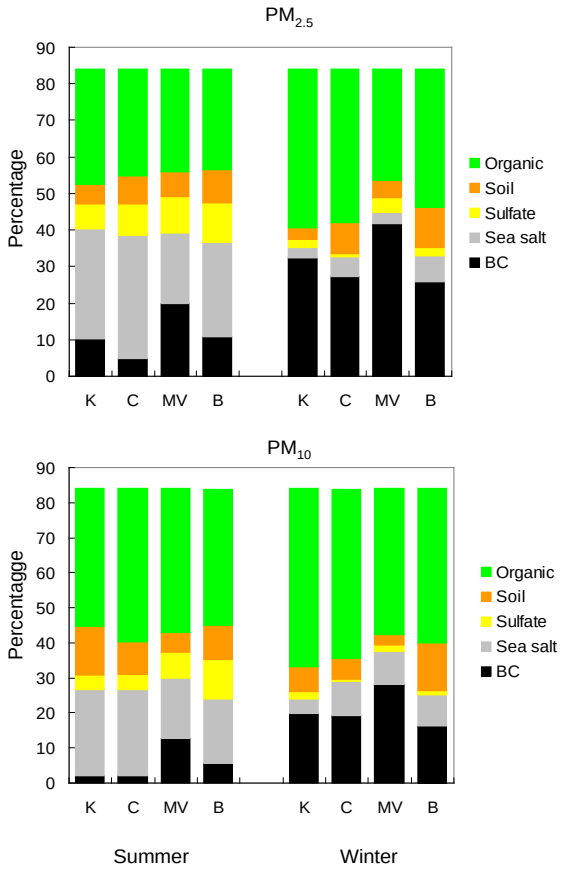

Figure 1 Average percentage of aerosol types for Kensington (K), Campbelltown (C), Moss Vale (MV) and Berrima (B) in summer (left) and winter (right).

The refractive indices used in these calculations were taken from the literature (Weast 1975, 1977; Stelson 1990; Morrison and Boyd 1978; Lide 1997; Evans 2003; Aylward and Findlay 2008). The refractive index for organics was assumed to be 1.4 (Turpin and Lim, 2001) and for black carbon it was assumed to be 1.5 (Lide, 1997). The imaginary component of refractive index of black carbon was taken as 0.47 (Horvath, 1993) because these particles occur as a mixture of soot and air. The reference refractive index of soluble substances (ions) was taken from the literature (Stelson, 1990; Moelwyn-Hughes, 1961).

Refractive index was determined for each day at each site (daily mass) and from these values seasonal and yearly averages were calculated. A second set of calculations was done using average chemistry (average mass) for the season or year, in order to determine whether or not using average chemistry has a significant effect on the result.

2.4 Sources of error

In order to use elemental chemistry as input to SCAPE 2 it was assumed that the ionic concentration was the same as the elemental concentration. However SCAPE 2 is based on soluble ions whereas total elemental concentration will include both soluble and insoluble fractions. Since no soluble ion chemistry was available to this study the uncertainty introduced by these assumptions was estimated using values for the Sydney region taken from the literature. Nitrates were assumed to be 8% of total mass (Cohen et al. 1995). Total carbonate concentration as H_2CO_3 was calculated using a CO_2 global average concentration of 360 ppm (Meng et al. 1995).

Ayers et al. (1999) measured both elemental and ion concentrations of aerosol samples in Sydney as part of the Australian Fine Particle study. For Na, Cl, K, Ca and S a multiplicative factor, the ratio of ion concentration to elemental concentration (from PIXE), was determined for both $PM_{2.5}$ and PM_{10}. These ratios are given in Table 1. The ion/element ratios for Na, Cl, K, Ca and S indicated that 95% of $PM_{2.5}$ and 68% of PM_{10} was soluble.

	IC/PIXE Ratio	
	$PM_{2.5}$	PM_{10}
Na	0.97	0.46
Cl	1.05	0.81
K	0.89	0.70
Ca	0.90	0.76
S	0.60	0.58

Table 1 Ratio of ion concentration to element concentration for Sydney aerosols

The low mass concentration of samples in this study meant that Mg was below the minimum detectable limit for IBA so was assumed to be zero in the SCAPE 2 runs. To estimate the level of error introduced by this assumption the concentration of soluble Mg ions was taken from Ayers et al. (1999) for both $PM_{2.5}$ and PM_{10}, while elemental Mg for $PM_{2.5}$ was taken from PIXE results for Christchurch obtained by Senaratne et al. (2005).

Two representative data sets were selected for the test, a $PM_{2.5}$ summer and PM_{10} winter. For both test data sets SCAPE 2 was run for ions input with and without Mg, and also elemental input data with Mg. Real refractive index was calculated for the test cases and these were compared with the original estimates. It was found that using the ions output without Mg resulted in a refractive index about 3% higher than with elements as input. When Mg is also included, the refractive index is approximately 10% higher.

3 Results

The primary purpose of this study was to determine the size-resolved refractive index for the Sydney region, including seasonal and spatial variations, which are discussed in Section 3.1. In Section 3.2 we illustrate some potential applications of this approach.

3.1 Refractive index

In this study measured elemental chemistry has been used to determine the size-resolved refractive index for the Sydney region and to examine its seasonal and spatial variations. For each sample the chemical compounds present have been derived from the elemental composition using both a chemical thermodynamic model and aerosol types. This resulted in two sets of refractive indices.

The analysis of the data was motivated by the following questions: 1) does seasonally averaged chemistry give reliable results; 2) are there seasonal or site variation in refractive index; 3) is refractive index based on aerosol types comparable to that based on the chemical thermodynamic model? To answer these questions the seasonal average and standard deviation of daily samples, referred to as daily mass, was calculated for each site. This was done for $PM_{2.5}$ and PM_{10} samples for both datasets. The final results of these calculations are summarised in Table 2. The full results are given in the Appendix, along with the corresponding refractive indices based on seasonally averaged chemistry (referred to as average mass).

3.1.1 Real component of refractive index

For each dataset the real refractive index based on seasonally averaged mass agreed with that based on daily mass within one standard deviation for both $PM_{2.5}$ and PM_{10} in the vast majority of cases. (See Appendix Table A for detailed results.) Comparison of $PM_{2.5}$ and PM_{10} seasonal refractive indices showed that the differences between sites, and also between seasons, were small and less than the seasonal error bars. This leads to the conclusion that seasonally averaged chemistry gives reliable estimates of real refractive index and that the seasonal and spatial variations were not significant.

Table 2 gives the average $PM_{2.5}$ and average PM_{10} refractive index over all sites and seasons for both SCAPE 2 and aerosol types. The $PM_{2.5}$ and PM_{10} refractive indices based on aerosol types are slightly smaller than for SCAPE 2 but the difference is not significant. Benko et al. (2009) obtained similar results for Central European background aerosol which showed no significant variation in refractive indices between the seasons.

	$PM_{2.5}$	PM_{10}	$PM_{10\text{-}2.5}$
Real component			
SCAPE 2	1.46 (0.07)	1.46 (0.07)	1.47 (0.09)
Aerosol Types	1.44 (0.01)	1.43 (0.01)	1.44 (0.02)
Imaginary component			
Summer			
All	0.05 (0.02)	0.02 (0.01)	0.01 (0.04)
Rural	0.03 (0.01)	0.01 (0.01)	0.01 (0.02)
Urban	0.08 (0.04)	0.05 (0.03)	0.02 (0.04)
Spring			
All	0.23 (0.05)	0.12 (0.04)	0.04 (0.06)

Table 2 Summary of refractive index results. Data are averages over all sites and seasons with standard deviations in parentheses. $PM_{2.5}$ and PM_{10}: particulate matter less than 2.5 and 10 μm aerodynamic diameter. $PM_{10\text{-}2.5}$ is particulate matter between 2.5 and 10 μm aerodynamic diameter.

Comparison of refractive indices calculated from aerosol types and those calculated from SCAPE 2 showed good agreement for seasonally averaged daily mass and average mass for all sites and seasons. The standard deviations for the aerosol types were smaller than for SCAPE 2 which may reflect the limited range of aerosol types plus the assumption of constant 16% total mass for [water + nitrates]. (Aerosol types allows only one sulphate for example, whereas SCAPE 2 allows several, however refractive indices for most compounds are in the range 1.50 ± 0.05 so the effect is small.)

3.1.2 Imaginary component of refractive index

Calculation of the imaginary component of the refractive index depends only on black carbon concentration and is the same for both aerosol types and SCAPE 2. Results are summarised in Table 2. (See Appendix Table B for detailed results.) In the vast majority of cases the imaginary refractive index based on seasonally averaged mass agreed with that based on daily mass within the seasonal error bars. There was significant seasonal variation in the imaginary part of the refractive index, some variation between sites, and also variation with size fraction. The lowest values at all sites occurred in summer and the highest in spring (and winter), and in most cases the PM_{10} value is lower than the $PM_{2.5}$ value. Table 2 shows the average refractive index over all sites for summer and spring for both $PM_{2.5}$ and PM_{10}. Refractive index averaged over all sites is significantly lower in summer than in spring for both $PM_{2.5}$ and PM_{10}. Also shown are the summer averages for the urban (Kensington and Campbelltown) and rural (Moss Vale and Berrima) sites. The urban refractive index was significantly lower than the rural for both $PM_{2.5}$ and PM_{10}. For spring there were no significant differences between urban and rural sites. The differences in imaginary refractive index with size fraction reflect the stronger contribution of black carbon to $PM_{2.5}$.

3.1.3 Size-resolved refractive index

From the results presented above it is evident that a good estimate of refractive index can be obtained using seasonally averaged chemistry for both $PM_{2.5}$ and PM_{10}. This suggests that using coarse mode chemistry obtained by subtracting seasonal $PM_{2.5}$ from seasonal PM_{10} to estimate coarse mode ($PM_{10\text{-}2.5}$) refractive index should provide useful results. The coarse mode ($PM_{10\text{-}2.5}$) refractive index was calculated for both SCAPE 2 and aerosol types and the error estimated as the square root of sum squares of the corresponding $PM_{2.5}$ and PM_{10} errors. The results for the coarse ($PM_{10\text{-}2.5}$) fractions are summarised in Table 2. (See Appendix Table C for detailed results.) There are some small seasonal variations in real refractive index between seasons and between sites for $PM_{10\text{-}2.5}$, most noticeably Kensington and Berrima, but these are unlikely to be significant. The real refractive index averaged over all sites is the same as the corresponding PM_{10} value for both SCAPE 2 and aerosol types.

There are slight variations in imaginary component of the refractive index for the coarse fraction and this is reflected in the slightly higher value in spring than summer shown in Table 2. $PM_{10-2.5}$ values are also lower than corresponding PM_{10}, particularly for spring. The imaginary component is higher for $PM_{2.5}$ than for $PM_{10-2.5}$, even when errors are accounted for, reflecting the greater contribution of black carbon to the fine fraction. The real component of $PM_{10-2.5}$ refractive index is 1.47 ± 0.09 throughout the year and the imaginary component is 0.01 ± 0.04 for summer and 0.04 ± 0.06 for spring.

The good agreement between the results derived from the two datasets suggests that estimating aerosol refractive index based on aerosol types can give reliable results and could be very useful when only elemental composition is available. For cases where there are sufficiently large data sets available more sophisticated analysis, using positive matrix factorisation for example, would allow more accurate determination of the aerosol types present. This in turn would allow more accurate estimates of refractive index for that location.

3.2 Application of Refractive Index Results

3.2.1 Aerosol scattering properties definitions

Aerosol optical properties which depend on aerosol refractive index include the extinction and scattering efficiencies, single scattering albedo and the asymmetry parameter. Brief definitions are given here and more details can be found in Box and Box (2016). The extinction efficiency, β_e, is a measure of the attenuation of the beam due to both absorption and scattering, while the scattering efficiency, β_s, is a measure of attenuation due to scattering. These are defined as:

$$\beta_i = \int \pi r^2 Q_i n(r) dr \qquad i = e, s \text{ for extinction and scattering respectively.}$$

Q_i is the Mie extinction or scattering coefficient and $n(r)$ is the aerosol size distribution. It should be noted that Q_i is a function of particle size, refractive index and wavelength.

The single scatter albedo ϖ provides a measure of how well a population of particles scatters incident light, $\varpi = 1$ for a perfect scatterer and $\varpi = 0$ for a perfect absorber. It is defined as:

$$\varpi = \beta_s / \beta_e$$

The asymmetry parameter g gives a measure of the directionality of the scattered beam, $g = 0$ being uniformly scattered in all directions and $g = 1$ being highly directional. It is defined as:

$$g = \beta_s^{-1} \int \pi r^2 g(r) Q_s n(r) dr$$

$g(r)$ is the asymmetry parameter for an individual particle of radius r.

The size distributions used to calculate the optical properties were modelled as bimodal lognormal distributions with a fine mode corresponding to $PM_{2.5}$ and a coarse mode corresponding to $PM_{10-2.5}$. Each mode has the form:

$$n(r) = \frac{N}{\sqrt{2\pi} r \ln \sigma} \exp\left\{ -0.5 \left(\frac{\ln r - \ln r_m}{\ln \sigma} \right)^2 \right\}$$

where $n(r)$ is the radius-number size distribution, N is the total number of particles per unit volume, r_m is the geometric mean radius and σ is the size distribution geometric standard deviation.

3.2.2 Aerosol scattering properties calculations

Aerosol optical properties depend on both refractive index and size distribution. In this section we examine the seasonal and spatial variations of aerosol scattering properties for the Sydney region. This illustrates a potential application of refractive index determination using aerosol chemistry.

A set of three size distributions was constructed based on measured size distributions for the Sydney area. This ensured that the values chosen for geometric mean radius (r_m) and geometric standard deviation (σ) for both fine and coarse modes were appropriate for Sydney. Model parameters were chosen to give one size distribution where the fine mode dominated the mass, one with roughly equal fine and coarse mass, and a third where the coarse mode dominated the total mass. The size distribution parameters and $PM_{2.5}/PM_{10}$ ratios are given in Table 3. The area-weighted distribution $r^2 n(r)$ (units: $\mu m^2\ \mu m^{-3}\ \mu m^{-1}$) is the most relevant representation for calculation of scattering properties and is illustrated in Figure 2.

	Coarse dominated	*Equal Mass*	*Fine dominated*
N_f (μm^{-3})	10^3	10^4	10^5
r_f (μm)	0.01	0.02	0.01
σ_f	2.5	2.5	2.5
N_c (μm^{-3})	1	10	0.5
r_c (μm)	0.12	0.10	0.15
σ_c	3.1	3.1	3.0
$PM_{2.5}/PM_{10}$	0.174	0.526	0.864

Table 3 Parameters for Aerosol Size distribution Models. N is number of particles per unit volume, r is geometric mean radius, σ is the geometric standard deviation, f and c denote fine and coarse mode respectively.

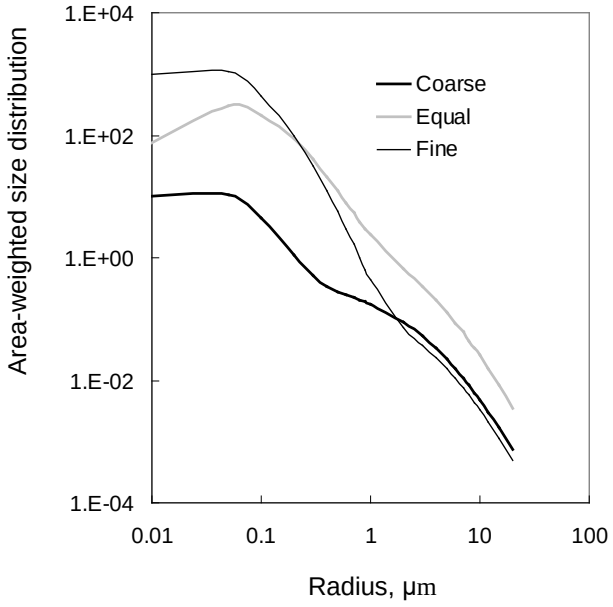

Figure 2 Area-weighted bimodal size distributions ($\mu m^2\ \mu m^{-3}\ \mu m^{-1}$). Coarse mass dominated is the solid black line, equal fine and coarse mass is the grey line, and fine mass dominated is the fine black line.

To examine variations in scattering properties the $PM_{2.5}$ and $PM_{10-2.5}$ summer and winter refractive indices for Kensington and Campbelltown were averaged to give representative seasonal urban values, and similarly Moss Vale and Berrima were averaged to give seasonal rural values. These refractive indices are given in Table 4. The variation of extinction, asymmetry parameter and single scattering albedo as a function of wavelength for each size distribution are illustrated in Figure 3.

	Fine mode ($PM_{2.5}$)		*Coarse mode ($PM_{10-2.5}$)*	
	Real	Imaginary	Real	Imaginary
Urban				
Summer	1.440	0.030	1.470	0.005
Winter	1.465	0.155	1.430	0.045
Rural				
Summer	1.445	0.065	1.485	0.020
Winter	1.525	0.145	1.430	0.055

Table 4 Size-resolved Refractive Indices for 4 cases.

It is evident from Figure 3 that the size distribution has an effect on the behaviour of scattering properties as a function of wavelength. The curves for the coarse mass dominated size distribution (left column) were the flattest and those for the fine mass dominated size distributions (right column) were the steepest.

Extinctions (top row) have been normalised to 1 at 0.5 μm to enable easy comparison of shape as a function of wavelength. There is very little difference between urban (black) and rural (grey) extinctions for a given size distribution but there are seasonal and size distribution differences. As noted above the coarse mass dominated size distribution is the flattest and there are no seasonal differences between normalised extinctions. For the other two size distributions the winter extinctions (dashed lines) are higher than summer (solid lines) at longer wavelengths and the effect is more pronounced for the fine mass dominated distribution.

The asymmetry parameter (middle row) shows seasonal, spatial and size distribution differences. For the coarse dominated size distribution the rural summer and winter asymmetry parameters are constant with wavelength at ≈ 0.8 while the urban values are slightly higher in winter and lower in summer. Seasonal and spatial differences for the size distribution with equal fine and coarse mass were small while for the fine mass dominated distribution asymmetry parameters decreased with wavelength and the effect was more pronounced for winter reflecting the increased absorption.

The seasonal, spatial and size distribution differences for single scatter albedo (bottom row) are most pronounced. A common feature for all three size distributions was that the difference between summer and winter values is greater for the urban case than for the rural case at all wavelengths. The summer urban values are higher than the rural ones, but the opposite is the case for winter.

4 Summary and Conclusion

In this paper we have used the aerosol chemistry for the Sydney region, presented in Hallal et al. (2003), to estimate size-resolved refractive index for Sydney. The chemical compounds present were determined from the elemental composition using two methods: the SCAPE 2 chemical thermodynamic model; and aerosol types based on marker elements. Refractive index was then calculated using a mass fraction approach. Representative refractive indices were then used to calculate aerosol scattering properties for three different size distributions to illustrate how this information could be used. The key findings are summarised below.

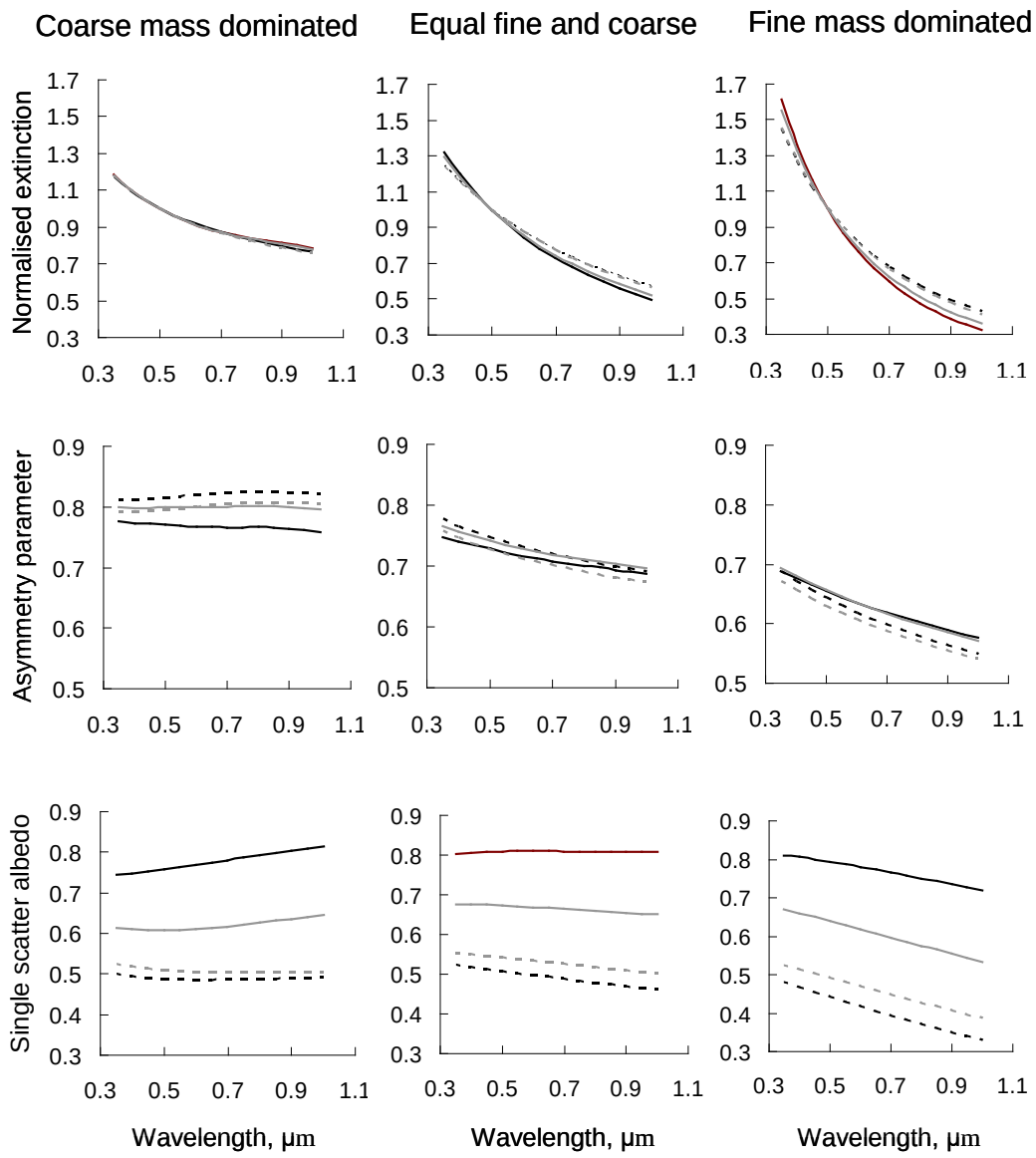

Figure 3. Aerosol scattering properties as a function of wavelength. Left column is properties for coarse mass dominated size distribution, middle column is equal fine and coarse mass, and right column is fine mass dominated. Black lines are for urban refractive indices and grey lines for rural refractive indices. Solid lines are summer and dashed lines are winter.

For both $PM_{2.5}$ and PM_{10} it was found that the results based on seasonally averaged chemistry were within one standard deviation of the seasonally averaged daily data, and generally much closer, indicating that averaged chemistry does lead to a representative value for refractive index.

- There was little seasonal or site variation in the real part of the refractive index which was found to be 1.46 ± 0.07 for both $PM_{2.5}$ and PM_{10}. The urban sites (Kensington and Campbelltown) tended to have slightly lower values than the rural sites (Moss Vale and Berrima) but the differences were not significant.
- The imaginary component of the refractive index showed strong variations with season, site and particle size. Lowest values were in summer and highest in spring. For $PM_{2.5}$ the summer average was 0.05 ± 0.02 (urban 0.03 ± 0.01, rural 0.08 ± 0.04) and the spring average was 0.23 ± 0.05. For PM_{10} the summer average was 0.02 ± 0.01 (urban 0.01 ± 0.01, rural 0.05 ± 0.03) while the spring average was 0.12 ± 0.04.

- The real part of the coarse mode ($PM_{10-2.5}$) refractive index showed little seasonal or site variation and was found to be 1.47 ± 0.09. This is the same as for $PM_{2.5}$ and PM_{10}. The imaginary component for the coarse mode was 0.01 ± 0.04 in summer and 0.04 ± 0.06 in spring. This was much lower than that for the fine mode and, unlike $PM_{2.5}$ and PM_{10}, seasonal and site variations were small and not significant. The lower imaginary component for $PM_{10-2.5}$ indicates that black carbon is predominantly in the fine mode.
- The values quoted above for real refractive index may be underestimates due to the assumptions made about the equivalence of elemental and ionic composition and the neglect of Mg. This source of error is of the order of 10%.
- Refractive indices based on aerosol types were comparable to those based on SCAPE 2 and indicate that using elemental composition to determine aerosol types, and thence refractive index, is a reliable approach.
- The most significant contributor to variations in refractive index (real and imaginary) is black carbon due to its strong seasonal variability. It should also be noted that there is a wide variation in refractive index for black carbon in the literature depending on its source, for example pure soot or a soot/air mixture, and mixture proportion. This will affect comparisons with other studies.

The results outlined above were used to calculate aerosol scattering properties for the Sydney region, specifically extinction, asymmetry parameter and single scatter albedo, as a function of wavelength. Three size distributions and four different refractive indices were used to investigate the effects of differing fine/coarse mode mass ratios as well as seasonal and spatial variations. Extinction decreased with wavelength for all three size distributions with the effect being strongest for the fine mass dominated distribution. Wavelength dependence of the asymmetry parameter and single scatter albedo was also strongest for the fine mass dominated distributions. Single scatter albedo showed the greatest variation between rural and urban sites, and also with season, for all three size distributions. Only extinction, single scattering albedo and asymmetry parameter were considered here because of large uncertainties in refractive index and the representative nature of the size distributions did not justify extending the application to more sophisticated radiative forcing calculations which would also require column loadings.

In this study elemental chemistry has been used to determine the refractive index for the Sydney region. We have demonstrated that the simplified method based on aerosol types gives comparable results to those based on the thermodynamic model. The simplified method may be preferable when only elemental composition data is available because it avoids introducing errors arising from assumptions about ion/element ratios. These assumptions affected the accuracy of the real part of the refractive index rather than the imaginary part which contributed most strongly to variability for the sites studied. There are separate issues regarding what values to use for black carbon refractive index and these will depend on local factors and sources.

This study has shown that useful information about aerosol optical properties can be derived from limited data. In this case fine and coarse mode refractive index was determined from elemental composition of aerosol samples collected on two low volume samplers ($PM_{2.5}$ and PM_{10}). Two major improvements to the procedure used here are recommended for future studies: a two-stage (or multi-stage) sampler, and high flow rate. In a two-stage sampler the same air passes through both stages separating the coarse and fine particles thus eliminating the major source of error arising from determination of the coarse mode by subtracting $PM_{2.5}$ from corresponding PM_{10}. A multi-stage sampler would allow for better size-resolution of chemistry and hence refractive index. High flow rates would lead to increased mass on filters resulting in more accurate elemental chemistry by ensuring that mass concentrations were above the minimum detectable limit for all elements.

Acknowledgments

The elemental chemistry analyses that formed the basis of this paper were done at ANSTO under AINSE grants AINGRA03178 and AINGRA08005.

References

Ayers, G.P., Keywood, M.D., Gras, J.L., Cohen, D.D., Garton, D. and Bailey, G.M. 1999. Chemical and physical properties of Australian fine particles: a pilot study. Final Report to Environment Australia from the Division of Atmospheric Research, CSIRO and the Australian Nuclear Science and Technology Organisation. CSIRO Australia.

Aylward, G. and Findlay, T. 2008. SI Chemical Data, 6th edition. John Wiley & Sons, Ltd. Milton, Queesland, Australia.

Benko, D., Molnar, A. and Imre, K. 2009. Study on the size dependence of complex refractive index of atmospheric aerosol particles over Central Europe. *IDŐJÁRÁS: Quarterly Journal of the Hungarian Meteorological Service*, 113(3), 157–175

Bond, T.C. and Bergstrom, R.W. 2006. Light absorption by carbonaceous particles: An investigative review. *Aerosol Sci. Tech*., 40(1), 27-67, doi:10.1080/027821521

Box, M.A. and Box, G.P., 2016. Physics of Radiation and Climate. CRC Press, Boca Raton, FL.

Cohen, D.D., Crisp, P.T. and Hyde, R. 1995. Contribution of fuel combustion to pollution by airborne particles in urban and non-urban environments. Report number ERDC 259, Energy Research and Development Corporation, Canberra.

Cohen, D.D., Stelcer, E., Hawas, O. and Garton, D. 2004. IBA methods for characterization of fine particulate atmospheric pollution: a local, regional and global research problem. *Nucl. Instrum. Meth. B*, 219-220, 145-152. doi:10.1016/JNIMB.2004.01.043

Evans, M.C.F. 2003. Characterization and formation of particulate nitrate in a coastal area. Department of Chemistry, College of Arts and Sciences, University of South Florida, USA

Hallal, T., Box, G.P., Cohen, D.D. and Stelcer, E. 2013. Size-resolved elemental composition of aerosol particles in greater Sydney in 2002-2003. *Environ. Chem*., 10, 295-305. doi:10.1071/EN121946820500

Hand, J.L. and Malm, W.C. 2007. Review of aerosol mass scattering efficiencies from ground-based measurements since 1990. *J. Geophys. Res*., 112, D16203, doi:10.1029/2007JD008484.

Horvath, H. 1993. Atmospheric light absorption – a review. *Atmos. Environ*. 27A, 293-317

Kim, Y.P., Seinfeld, J.H. and Saxena, P. 1993a. Atmospheric gas-aerosol equilibrium I. Thermodynamic model. *Aerosol Sci. Technol*., 19, 157-181

Kim, Y.P., Seinfeld, J.H. and Saxena, P. 1993b. Atmospheric gas-aerosol equilibrium II. Analysis of common approximation and activity coefficient calculation methods. *Aerosol Sci. Technol.*, 19, 182-198

Kim, Y.P. and Seinfeld, J.H. 1995. Atmospheric Gas-Aerosol Equilibrium III. Thermodynamics of Crustal Elements Ca2+, K+, and Mg2+. *Aerosol Sci. Technol*., 22, 93-110

Lide, D.R., 1997. Handbook of Chemistry and Physics. CRC Press, Boca Raton, FL.

Malm, W.C., Sisler, J.F., Huffman, D., Eldred, R.A. and Cahill T.A. 1994. Spatial and seasonal trends in particle concentration and optical extinction in the United States. *J. Geophys. Res*., 99, 1347-1370. doi: 10.1029/93JD00916

Meng, Z., Saxena, P. and Kim Y.P. 1995. Atmospheric gas-aerosol equilibrium IV. Thermodynamic of carbonates. *Aerosol Sci. Technol.*, 23, 131-154

Moelwyn-Hughes, E.A. 1961. Physical Chemistry, 2nd revised ed., Pergamon Press, New York, 397-400

Morrison, R.T. and Boyd R.N. 1978. Organic Chemistry, 3rd ed., New York University, Allyn and Bacon Inc., USA

Senaratne, I., Kelliher, F.M. and Triggs, C. 2005. Source apportionment of airborne particles during winter in contrasting coastal cities. *Aerosol and Air Quality Research*, 5(1), 48-64.

Stelson, A.W. 1990. Urban aerosol refractive index prediction by partial molar refraction approach. *Environ. Sci. Technol*. 24, 1676-1679

Taha, G., Cohen, D.D., Stelcer, E. and Box, G.P. 2007. Black carbon measurement using Laser Integrating Plate Method. *Aerosol Sci. Tech*., 41, 266-276. doi:10.1080/02786820601156224

Turpin, B.J. and Lim, H.J. 2001. Species contributions to PM2.5 mass concentrations: Revisiting common assumptions for estimating organic mass. *Aerosol Sci. Technol*., 35, 602-610.

Weast, R.C. 1975. Handbook of Chemistry and Physics, 56th ed. CRC Press, Cleveland, Ohio

Weast, R.C. 1977. Handbook of Chemistry and Physics, 57th ed. CRC Press, Cleveland, Ohio

5 Appendix

Table A Seasonal and yearly real refractive index. Data are as follows: averages, standard deviations in parentheses. $PM_{2.5}$ and PM_{10}: particulate matter less than 2.5 and 10 μm aerodynamic diameter.

	PM2.5				PM10			
	SCAPE 2		Aerosol Types		SCAPE 2		Aerosol Types	
	Daily Mass	Average Mass	Daily Mass	Average Mass	Daily Mass	Average Mass	Daily Mass	Average Mass
Kensington								
Summer	1.46 (0.06)	1.44	1.45 (0.01)	1.46	1.46 (0.08)	1.52	1.45 (0.01)	1.45
Autumn	1.46 (0.03)	1.46	1.44 (0.01)	1.44	1.44 (0.06)	1.52	1.42 (0.02)	1.44
Winter	1.43 (0.01)	1.47	1.43 (0.01)	1.44	1.46 (0.03)	1.46	1.43 (0.02)	1.43
Spring	1.46 (0.02)	1.47	1.44 (0.01)	1.44	1.44 (0.01)	1.46	1.43 (0.01)	1.43
Year	1.45 (0.06)	1.44	1.44(0.01)	1.46	1.45 (0.08)	1.49	1.43 (0.02)	1.45
Campbelltown								
Summer	1.43 (0.04)	1.44	1.46 (0.01)	1.46	1.45 (0.07)	1.44	1.44 (0.03)	1.44
Autumn	1.46 (0.04)	1.52	1.44 (0.01)	1.45	1.46 (0.03)	1.49	1.43 (0.01)	1.44
Winter	1.47 (0.04)	1.46	1.44 (0.01)	1.44	1.42 (0.04)	1.41	1.43 (0.01)	1.43
Spring	1.47 (0.03)	1.49	1.44 (0.02)	1.44	1.46 (0.02)	1.46	1.43 (0.01)	1.44
Year	1.46 (0.06)	1.42	1.44 (0.02)	1.46	1.45 (0.08)	1.43	1.44 (0.02)	1.45
Moss Vale								
Summer	1.45 (0.01)	1.45	1.45 (0.01)	1.46	1.45 (0.01)	1.43	1.44 (0.00)	1.45
Autumn	1.49 (0.05)	1.51	1.44 (0.01)	1.45	1.42 (0.04)	1.44	1.43 (0.02)	1.43
Winter	1.47 (0.01)	1.48	1.45 (0.02)	1.45	1.47 (0.02)	1.47	1.44 (0.02)	1.44
Spring	1.47 (0.02)	1.47	1.45 (0.01)	1.45	1.45 (0.01)	1.45	1.43 (0.00)	1.43
Year	1.47 (0.05)	1.48	1.45 (0.01)	1.45	1.44 (0.05)	1.48	1.43 (0.01)	1.44
Berrima								
Summer	1.45 (0.07)	1.46	1.46 (0.01)	1.46	1.49 (0.01)	1.48	1.45 (0.00)	1.45
Autumn	1.48 (0.01)	1.47	1.45 (0.02)	1.45	1.48 (0.04)	1.52	1.43 (0.02)	1.43
Winter	1.47 (0.04)	1.57	1.44 (0.00)	1.46	1.56 (0.05)	1.52	1.44 (0.01)	1.44
Spring	1.48 (0.01)	1.60	1.44 (0.01)	1.44	1.51 (0.02)	1.55	1.43 (0.01)	1.43
Year	1.47 (0.07)	1.55	1.45 (0.01)	1.46	1.51 (0.08)	1.49	1.44 (0.01)	1.44

Table B Seasonal and yearly Imaginary Refractive Index . Data are as follows: averages, standard deviations in parentheses. $PM_{2.5}$ and PM_{10}: particulate matter less than 2.5 and 10 μm aerodynamic diameter

	$PM_{2.5}$		PM_{10}	
	Daily Mass	Average Mass	Daily mass	Average mass
Kensington				
Summer	0.05 (0.02)	0.04	0.01 (0.01)	0.01
Autumn	0.14 (0.06)	0.11	0.02 (0.01)	0.02
Winter	0.19 (0.03)	0.19	0.09 (0.02)	0.15
Spring	0.25 (0.03)	0.24	0.10 (0.05)	0.16
Yearly	0.15 (0.12)	0.07	0.06 (0.07)	0.03
Campbelltown				
Summer	0.02 (0.01)	0.02	0.01 (0.01)	0.01
Autumn	0.14 (0.03)	0.13	0.09 (0.03)	0.09
Winter	0.11 (0.06)	0.12	0.08 (0.05)	0.07
Spring	0.19 (0.06)	0.17	0.15 (0.03)	0.14
Yearly	0.11±0.13	0.06	0.07 (0.08)	0.02
Moss Vale				
Summer	0.12 (0.08)	0.08	0.07 (0.04)	0.04
Autumn	0.10 (0.01)	0.09	0.10 (0.06)	0.08
Winter	0.25 (0.05)	0.24	0.16 (0.07)	0.15
Spring	0.31 (0.04)	0.28	0.18 (0.02)	0.20
Yearly	0.18 (0.16)	0.15	0.13 (0.11)	0.11
Berrima				
Summer	0.05 (0.01)	0.05	0.03 (0.01)	0.03
Autumn	0.24 (0.03)	0.23	0.08 (0.04)	0.07
Winter	0.11 (0.02)	0.05	0.05 (0.03)	0.05
Spring	0.18 (0.07)	0.16	0.06 (0.02)	0.03
Yearly	0.13 (0.14)	0.09	0.06 (0.05)	0.07

Table C Size-resolved Refractive Index . Data are as follows: averages, errors in parentheses. $PM_{2.5}$ particulate matter less than 2.5 μm aerodynamic diameter (fine fraction), $PM1_{0\text{-}2.5}$ (coarse fraction). $PM_{10\text{-}2.5}$ errors are sum of $PM_{2.5}$ and PM_{10} in quadrature.

		Real		*Imaginary*	
	SCAPE 2		Aerosol Types		
	$PM_{2.5}$	$PM_{10\text{-}2.5}$	$PM_{10\text{-}2.5}$	$PM_{2.5}$	$PM_{10\text{-}2.5}$
Kensington					
Summer	1.44 (0.06)	1.50 (0.10)	1.45 (0.01)	0.04 (0.02)	0.00 (0.02)
Autumn	1.46 (0.03)	1.54 (0.07)	1.42 (0.02)	0.11 (0.06)	0.01 (0.06)
Winter	1.47 (0.01)	1.47 (0.03)	1.43 (0.02)	0.19 (0.03)	0.07 (0.04)
Spring	1.47 (0.02)	1.49 (0.02)	1.43 (0.01)	0.24 (0.03)	0.05 (0.06)
Yearly	1.44 (0.06)	1.52 (0.10)	1.43 (0.02)	0.07 (0.12)	0.01 (0.14)
Campbelltown					
Summer	1.44 (0.04)	1.44 (0.08)	1.43 (0.03)	0.02 (0.01)	0.01 (0.01)
Autumn	1.52 (0.04)	1.42 (0.05)	1.47 (0.01)	0.13 (0.03)	0.03 (0.04)
Winter	1.46 (0.04)	1.39 (0.06)	1.47 (0.01)	0.12 (0.06)	0.02 (0.08)
Spring	1.49 (0.03)	1.46 (0.04)	1.47 (0.02)	0.17 (0.06)	0.05 (0.07)
Yearly	1.42 (0.06)	1.43 (0.10)	1.45 (0.03)	0.06 (0.13)	0.01 (0.15)
Moss Vale					
Summer	1.45 (0.01)	1.44 (0.01)	1.44(0.01)	0.08 (0.08)	0.03 (0.09)
Autumn	1.51 (0.05)	1.42 (0.06)	1.46 (0.02)	0.09 (0.01)	0.07 (0.06)
Winter	1.48 (0.01)	1.42 (0.02)	1.42(0.03)	0.24 (0.05)	0.08 (0.09)
Spring	1.47 (0.02)	1.43 (0.02)	1.41(0.01)	0.28 (0.04)	0.06 (0.04)
Yearly	1.48 (0.05)	1.44 (0.07)	1.44 (0.01)	0.15 (0.16)	0.04 (0.19)
Berrima					
Summer	1.46 (0.07)	1.53 (0.01)	1.46(0.01)	0.05 (0.01)	0.01 (0.01)
Autumn	1.47 (0.01)	1.60 (0.04)		0.23 (0.03)	0.00 (0.05)
Winter	1.57 (0.04)	1.44 (0.06)	1.44(0.01)	0.05 (0.02)	0.03 (0.04)
Spring	1.60 (0.01)	1.58 (0.02)	1.44(0.01)	0.16 (0.07)	0.01 (0.07)
Yearly	1.55 (0.07)	1.49 (0.11)	1.44 (0.01)	0.09 (0.14)	0.02 (0.15)